Journal of the Iranian Chemical Society
https://doi.org/10.1007/s13738-020-01854-w

SHORT COMMUNICATION

Iridium nanoparticles deposited on hypercrosslinked polystyrene: synthesis and application in the hydrogenation of aromatic compounds

Sergey E. Lyubimov[1] · **Marina V. Sokolovskaya**[1] · **Alexander A. Korlyukov**[1] · **Oleg P. Parenago**[2] · **Vadim A. Davankov**[1]

Received: 15 October 2019 / Accepted: 3 January 2020

Abstract

A novel method for the incorporation of iridium nanoparticles into a hypercrosslinked polystyrene matrix is developed using supercritical CO_2 as reaction medium. The composite has regularly distributed iridium nanoparticles with monomodal size of ca 5 nm. The catalyst shows high activity in the hydrogenation of benzene and can be recycled ten times without any decrease in productivity. The catalyst gave a full conversion in the hydrogenation of toluene to methylcyclohexane and fluoro- and chlorobenzene to cyclohexane.

Keywords Hypercrosslinked polystyrene · Iridium nanoparticles · Hydrogenation · Arenes

Introduction

New methods for the synthesis of metal nanoparticles have attracted increased attention because of their inherent large surface-to-volume ratio and quantum size effects [1–5]. The high surface area and thereby large number of active centers make the metal nanoparticle dispersions very attractive for catalysis application [6, 7]. Nevertheless, these ultrafine particles often agglomerate to form either lumps or secondary larger particles in order to minimize the total surface or the interfacial energy of the system [8–10]. Therefore, it is very important to stabilize the nanoparticles against adverse agglomeration at preparation, storage and usage stages. The use of stabilizing agents such as surfactants, ionic liquids, polyoxoanions, carbon nanotubes and polymers provides metal nanoparticles stabilized by electronic and/or steric protection [11–18]. It should be noted that the catalytic activity of heterogeneous catalysts depends not only on its stability but also on the accessibility of their surface area to the reacting molecules. One advanced polymeric support characterized by very high specific surface area (typically in the range of 1000 m^2/g) is hypercrosslinked polystyrene (HPS) [19]. Moreover, HPS polymers can swell in a wide range of solvents, even thermodynamically poor ones. Accordingly, Pt, Pd or Ru nanoparticles incorporated into a HPS matrix were successfully used in the oxidation, cross-coupling, hydroformylation and hydrogenation reactions [20–24].

Among the nanosized transition metals commonly used in catalysis, synthesis of iridium nanoparticles is limited to a few examples. Different supports, such as ionic liquids, silica, carbon nanotubes, alumina and polyvinylpyrrolidone, have been studied to immobilize Ir nanoparticles [11, 25–30].

Here we report a new method for the formation of Ir nanoparticles in HPS matrix, which consist of decomposition-reduction of $[Ir(COD)Cl]_2$ in supercritical CO_2/H_2, as well as a successful use of the composite in the hydrogenation of benzene, toluene, fluorobenzene and chlorobenzene.

Electronic supplementary material The online version of this article (https://doi.org/10.1007/s13738-020-01854-w) contains supplementary material, which is available to authorized users.

✉ Sergey E. Lyubimov
lssp452@mail.ru

[1] A.N. Nesmeyanov Institute of Organoelement Compounds, Russian Academy of Sciences, Vavilov Str. 28, Moscow, Russia 119991

[2] Institute of Petrochemical Synthesis, Russian Academy of Sciences, Leninsky Prospekt 29, Moscow, Russia 119991

Experimental part

General

Biporous (characteristic pore size 71 and 1.6 nm) support (insoluble in organic and inorganic solvents 0.3–1.2 mm beads), hypercrosslinked polystyrene Macronet™ MN-200 with the specific surface area of 1100 m^2/g (Purolite, UK) was washed with MeOH and dried in vacuo before the use. $[Ir(COD)Cl]_2$ (Sigma-Aldrich) was used as received. Samples morphology was studied using Hitachi HT7700 transmission electron microscope. Images were acquired in bright-field TEM mode at 100 kV accelerating voltage. X-ray powder diffraction (XRD) patterns were taken by a Bruker D8 Advanced X-ray diffractometer using CuKa radiation ($\lambda = 1.5406$ Å). ^1H NMR spectra were recorded on a Bruker 400 spectrometer in $CDCl_3$. X-ray fluorescence analysis was performed on an Innov-X α-2000 X-Ray spectrometer.

Catalyst preparation

$[Ir(COD)Cl]_2$ (64 mg) was dissolved in CH_2Cl_2 (5.4 mL) and added to industrial Macronet MN-200 resin (0.7 g); the solvent was removed in vacuo. The resin was placed into a 10-mL stainless-steel autoclave and the vessel was pressurized with H_2 (45 atm) and then filed with CO_2 by means of a syringe press (High Pressure Equipment) to the total pressure of 150 atm. The mixture was heated for 45 min (50 °C) and then slowly depressurized. A gray composite was washed by acetone (3 × 5 mL) and dried in vacuo.

General procedure for arene hydrogenation

76 mg of the polymer-Ir composite was placed into a stainless-steel autoclave, and 4.43 mmol of arene was added. The autoclave was filled with H_2 (45 atm) and maintained for 5 or 24 h (25 or 100 °C), cooled to 25 °C and then depressurized. The liquid reaction mixture was separated from the solid catalyst using a Pasteur pipette and analyzed by ^1H NMR. For reuse experiments, 0.4 mL of benzene and 45 atm H_2 were added again and the autoclave was heated for 5 h.

Results and discussion

The Ir(0) nanoparticles immobilized in Purolite Macronet MN-200 resin were obtained by adsorption of $[Ir(COD)Cl]_2$ dissolved in CH_2Cl_2, followed by vacuum draying and reduction with hydrogen in supercritical CO_2. According to X-ray fluorescence analysis, the average iridium content in the resin was found to be 2.8%. The powder X-ray diffraction measurement showed diffraction peaks 2θ at of 40.7°, 47.3° and 69.1° which correspond to face-centered-cubic crystalline structure of the Ir nanoparticles (Fig. 1) [31]. Calculation of crystallite size from integral breadth of reflections using L_{vol}-IB formalism showed that the average size of the Ir nanoparticles amounts to 0.5 nm. Such a low value of crystallite size can be explained by weak diffraction of iridium nanoparticles that faded by scattering from amorphous polystyrene.

The size and morphology of the Ir(0) nanoparticles were also investigated by TEM analysis of the milled MN-200 resin-iridium composite (Fig. 2). The nanoparticles were enough regularly distributed and have monomodal size of ca 6 nm. The histogram of nanoparticle

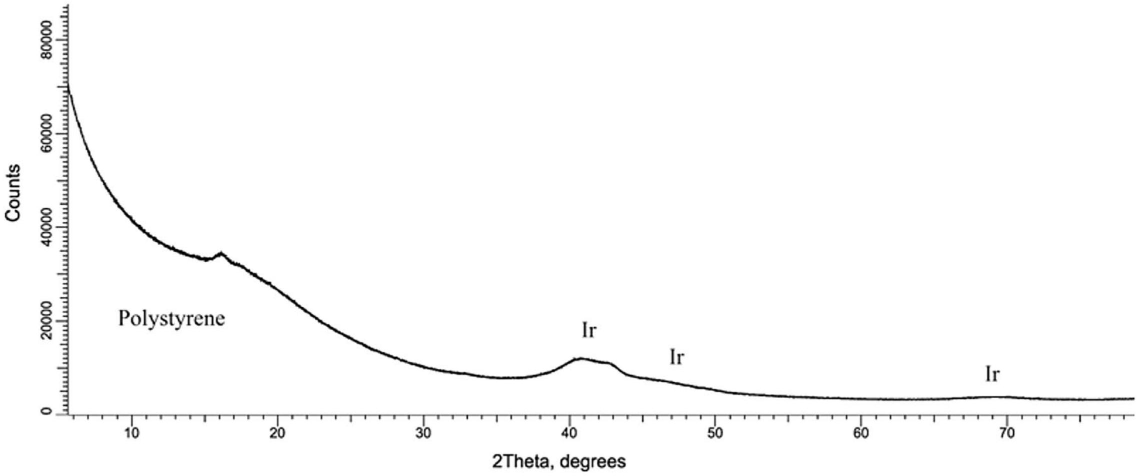

Fig. 1 XRD patterns of the catalyst

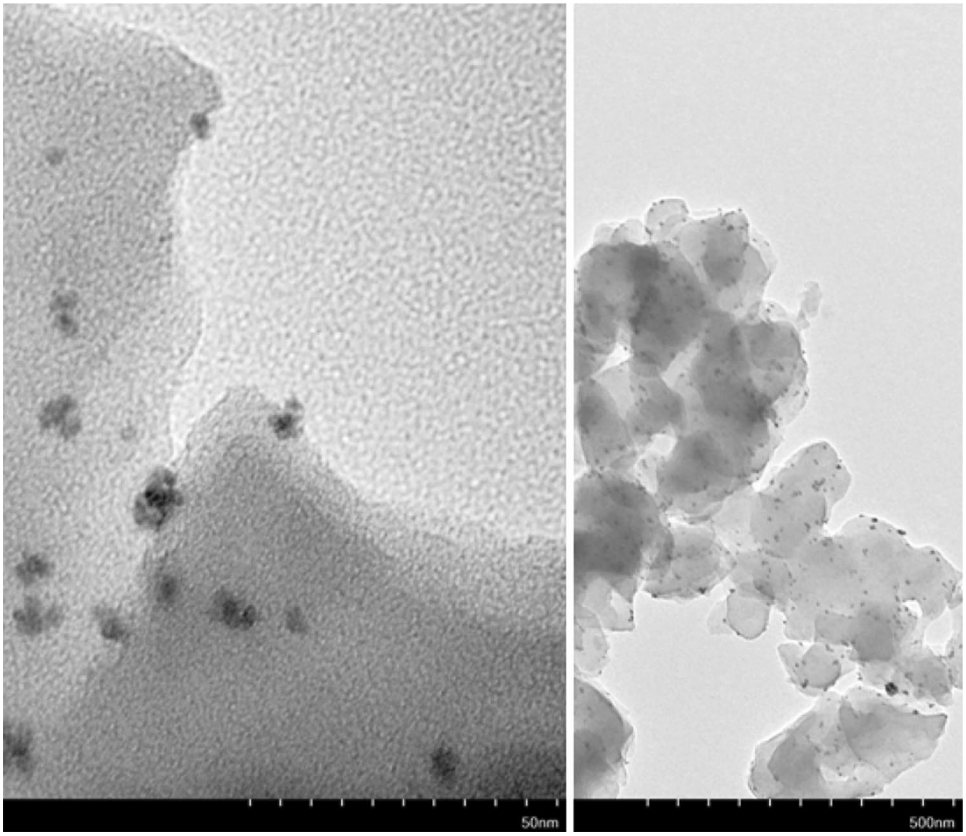

Fig. 2 TEM image of the milled catalyst

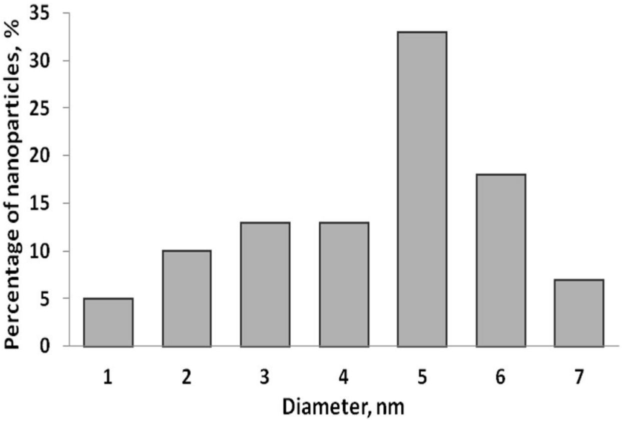

Fig. 3 Nanoparticles distribution histogram

distribution is represented in Fig. 3. Interestingly that each particle exists as a non-spherical shape-cluster.

The obtained iridium composite was tested as a hydrogenation catalyst for some model aromatic hydrocarbons. The HPS-based system was first used for benzene hydrogenation yielding cyclohexane which is commonly used as a non-toxic solvent. At 45 atm H_2 and 25 °C, conversion was 99.8% using only 0.25 mol% of iridium (Table 1, entry 1). Lowering of H_2 pressure led to a decrease in the reaction rate (Table 1, entry 2).

The use of a higher reaction temperature (100 °C) gave full conversion of benzene in 5 h (Table 1, entry 3). To test the reusability of the catalyst, a series of twelve consecutive runs were carried out. A complete conversion was obtained in ten catalytic cycles, but decreased starting with the eleventh catalytic run (Table 1, entries 3–14).

We have also examined the hydrogenation of toluene, chlorobenzene, fluorobenzene and aniline. In the case of toluene full conversion to methylcyclohexane was obtained in 5 h at 100 °C (Table 1, entry 15). Under the same conditions, chlorobenzene and fluorobenzene were exposed to hydrodehalogenation process forming cyclohexane as the only product (Table 1, entry 16, 17). Accordingly, the process may be interesting to utilize toxic, thermally stable and ozone depleting aryl halides to the harmless cyclohexane after synthetic use [32, 33]. In the case of aniline, the catalyst gave a moderate conversion to aminocyclohexane, probably due to deactivation of nanoparticles by the strongly coordination active substrate (Table 1, entry 18).

Table 1 Hydrogenation of arenes

Entry	Substrate	Cycle	P_{H2}, atm	*T*, °C	*t*, h	Conversion, %
1	Benzene	–	45	25	24	99.8
2	Benzene	–	10	25	24	72
3	Benzene	1	45	100	5	100
4	Benzene	2	45	100	5	100
5	Benzene	3	45	100	5	100
6	Benzene	4	45	100	5	100
7	Benzene	5	45	100	5	100
8	Benzene	6	45	100	5	100
9	Benzene	7	45	100	5	100
10	Benzene	8	45	100	5	100
11	Benzene	9	45	100	5	100
12	Benzene	10	45	100	5	100
13	Benzene	11	45	100	5	70
14	Benzene	12	45	100	5	30
15	Toluene	–	45	100	5	100
16	Chlorobenzene[a]	–	45	100	5	100
17	Fluorobenzene[a]	–	45	100	5	100
18	Aniline	–	45	100	5	20

Ir—0.25% mol

[a] Cyclohexane obtained as the only product

Conclusions

We report a novel rapid method for obtaining a reusable Ir(0) catalyst by decomposition-reduction of $[Ir(COD)Cl]_2$ in supercritical CO_2/H_2 within the matrix of hypercrosslinked polystyrene. The method allows obtaining composite with regularly distributed iridium nanoparticles having monomodal size of ca 5 nm. The HPS/Pd composite showed high activity in the hydrogenation of benzene and can be recycled ten times without any decrease in productivity. The catalyst gave a full conversion in the hydrogenation of toluene to methylcyclohexane and fluoro- and chlorobenzene to cyclohexane. Accordingly, the last process may be interesting to utilize toxic, thermal stable and ozone depleting aryl halides to the harmless cyclohexane after synthetic use.

Acknowledgements This work was supported by Russian foundation for basic research, Grant No. 18-29-06032. Authors thank the Department of structural studies of Zelinsky Institute of organic chemistry (Moscow) for electron microscopy characterization.

References

1. C. Amiensa, D. Ciuculescu-Pradines, K. Philippot, Coord. Chem. Rev. **308**, 409–432 (2016)
2. S.J.T. Rezaei, A. Shamseddin, A. Ramazani, A.M. Malekzadeh, P.A. Asiabi, Appl. Organomet. Chem. **31**, 1–10 (2017)
3. J. Dupont, J.D. Scholten, Chem. Soc. Rev. **39**, 1780–1804 (2010)
4. N. Yan, C.X. Xiao, Y. Kou, Coord. Chem. Rev. **254**, 1179–1218 (2010)
5. R. Mirsafaei, M.M. Heravi, T. Hosseinnejad, S. Ahmadi, Appl. Organomet. Chem. **30**, 823–830 (2016)
6. G. Schmid, Chem. Rev. **92**, 1709–1727 (1992)
7. O.A. Belyakova, Y.L. Slovokhotov, Russ. Chem. Bull. **52**, 2299–2327 (2003)
8. M.A. Gelesky, A.P. Umpierre, G. Machado, R.R.B. Correia, W.C. Magno, J. Morais, G. Ebeling, J. Dupont, J. Am. Chem. Soc. **127**, 4588–4589 (2005)
9. D. Astruc, F. Lu, J.R. Aranzaes, Angew. Chem. Int. Ed. **44**, 7852–7872 (2005)
10. C. Pan, K. Pelzer, K. Philippot, B. Chaudret, F. Dassenoy, P. Lecante, M.J. Casanove, J. Am. Chem. Soc. **123**, 7584–7593 (2001)
11. C.A. Stowell, B.A. Korgel, Nano Lett. **5**, 1203–1207 (2005)
12. A. Roucoux, J. Schulz, H. Patin, Adv. Synth. Catal. **345**, 222–229 (2003)
13. J.D. Aiken, Y. Lin, R.G. Finke, J. Mol. Catal. A: Chem. **114**, 29–51 (1996)
14. J.A. Widegren, J.D. Aiken, S. Ozkar, R.G. Finke, Chem. Mater. **13**, 312–324 (2001)
15. J.L. Pellegatta, C. Blandy, V. Colliere, R. Choukroun, B. Chaudret, P. Cheng, K. Philippot, J. Mol. Catal. A: Chem. **178**, 55–61 (2002)
16. H.J. Ryu, L. Sanchez, H.A. Keul, A. Raj, M.R. Bockstaller, Angew. Chem. Int. Ed. **47**, 7639–7643 (2008)
17. Y. Hu, Y.Y. Yu, Z.S. Hou, H. Li, X.G. Zhao, B. Feng, Adv. Synth. Catal. **350**, 2077–2085 (2008)
18. R.M. Esteban, K. Schütte, P. Brandt, D. Marquardt, H. Meyer, F. Beckert, R. Mülhaupt, H. Kölling, C. Janiak, Nano-Struct. Nano-Objects **2**, 11–18 (2015)
19. L. Tan, B. Tan, Chem. Soc. Rev. **46**, 3322–3356 (2017)
20. E. Sulman, V. Matveeva, L. Bronstein, A. Sidorov, N. Lakina, S. Sidorov, P. Valetsky, Green Chem. **5**, 205–208 (2003)

21. E. Sulman, V. Doluda, S. Dzwigaj, E. Marceau, L. Kustov, O. Tkachenko, A. Bykov, V. Matveeva, M. Sulman, N. Lakina, J. Mol. Catal. A: Chem. **278**, 112–119 (2007)
22. E.M. Sulman, A.A. Ivanov, V.S. Chernyavsky, M.G. Sulman, A.I. Bykova, A.I. Sidorov, VYu. Doluda, V.G. Matveeva, L.M. Bronstein, B.D. Stein, A.S. Kharitonov, Chem. Eng. J. **176–177**, 33–41 (2011)
23. S.E. Lyubimov, A.A. Vasil'ev, A.A. Korlyukov, M.M. Ilyin, S.A. Pisarev, V.V. Matveev, A.E. Chalykh, S.G. Zlotin, V.A. Davankov, React. Funct. Polym. **69**, 755–758 (2009)
24. S.E. Lyubimov, E.A. Rastorguev, K.I. Lubentsova, A.A. Korlyukov, V.A. Davankov, Tetrahedron Lett. **54**, 1116–1119 (2013)
25. J. Dupont, G.S. Fonseca, A.P. Umpierre, P.F.P. Fichtner, S.R. Teixeira, J. Am. Chem. Soc. **124**, 4228–4229 (2002)
26. G.S. Fonseca, A.P. Umpierre, P.F.P. Fichtner, S.R. Teixeira, J. Dupont, Chem. Eur. J. **9**, 3263–3269 (2003)
27. S. Kundu, H. Liang, J. Colloid Interface Sci. **354**, 597–606 (2011)
28. Y. Lin, R.G. Finke, Inorg. Chem. **33**, 4891–4910 (1994)
29. B.J. Hornstein, R.G. Finke, Chem. Mater. **15**, 899–909 (2003)
30. A. Goel, N. Rani, Open J. Inorg. Chem. **2**, 67–73 (2012)
31. L. Fu, X. Zeng, C. Huang, P. Cai, G. Cheng, W. Luo, Inorg. Chem. Front. **5**, 1121–1125 (2018)
32. E.C. Butler, K.F. Hayes, Environ. Sci. Technol. **33**, 2021–2027 (1999)
33. E.D. Goldberg, Sci. Total Environ. **100**, 17–28 (1991)